Supporting Information

Elucidating Pt-based Nanocomposite Catalysts for the Oxygen Reduction Reaction in Rotating Disk Electrode and Gas Diffusion Electrode measurements

Jia Du[a], Jonathan Quinson[b], Alessandro Zana[a], Matthias Arenz[a] *

[a] Department of Chemistry and Biochemistry, University of Bern, Freiestrasse 3, 3012 Bern, Switzerland

[b] Department of Chemistry, University of Copenhagen, Universitetsparken 5, 2100 Copenhagen Ø, Denmark

* corresponding author: matthias.arenz@dcb.unibe.ch

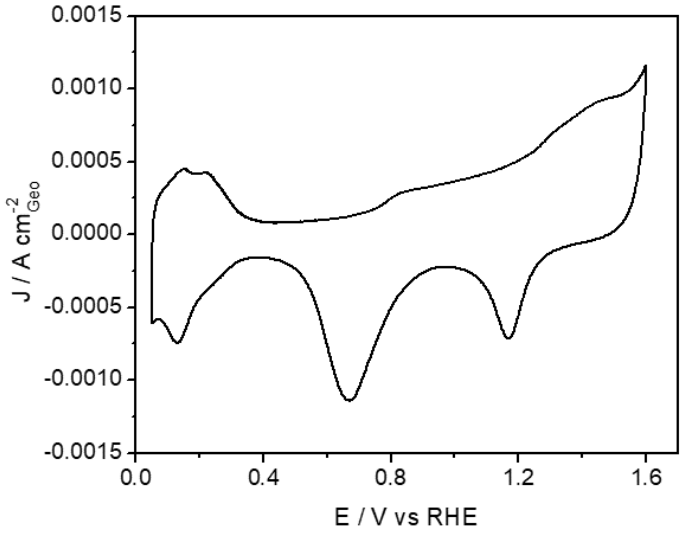

Figure S1. CV of the Pt-Au/C nanocomposite recorded at room temperature in $HClO_4$ aqueous electrolyte. The scan rate was 50 mV s^{-1}.

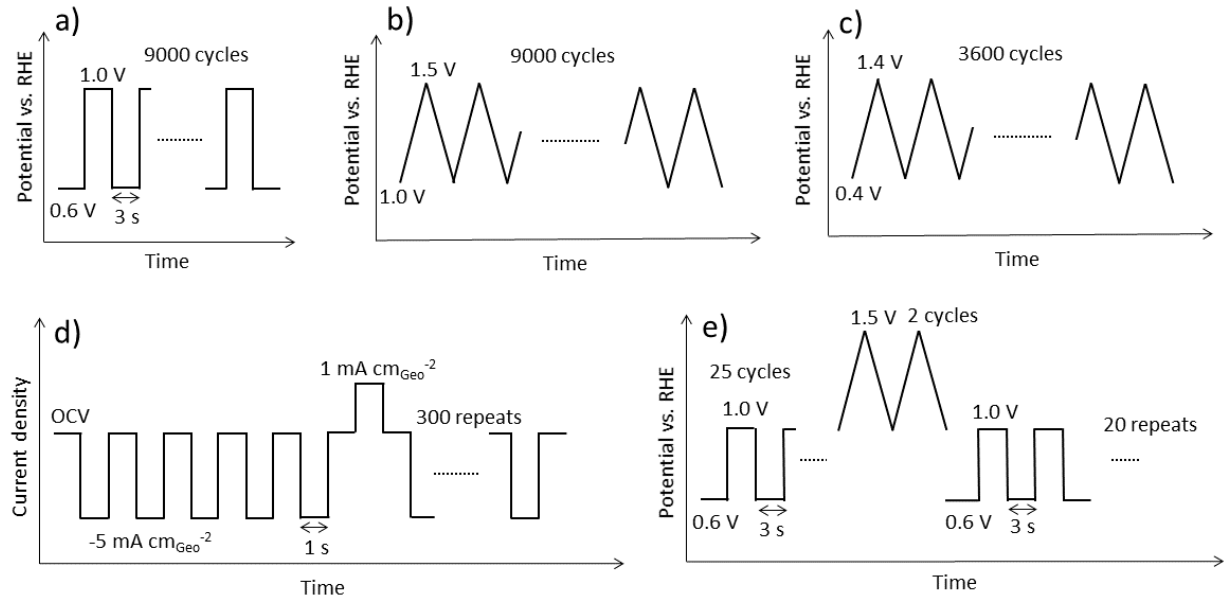

Figure S2. Schemes of the different applied ADT protocols in the RDE (a, b, c and d) and the GDE (e) measurements. The protocols of the RDE measurements were performed in Ar atmosphere (a, b and c) as well as O_2 atmosphere (d), while the protocol with a mixture of potential holding and potential cycling of the GDE measurement were performed in O_2 atmosphere.

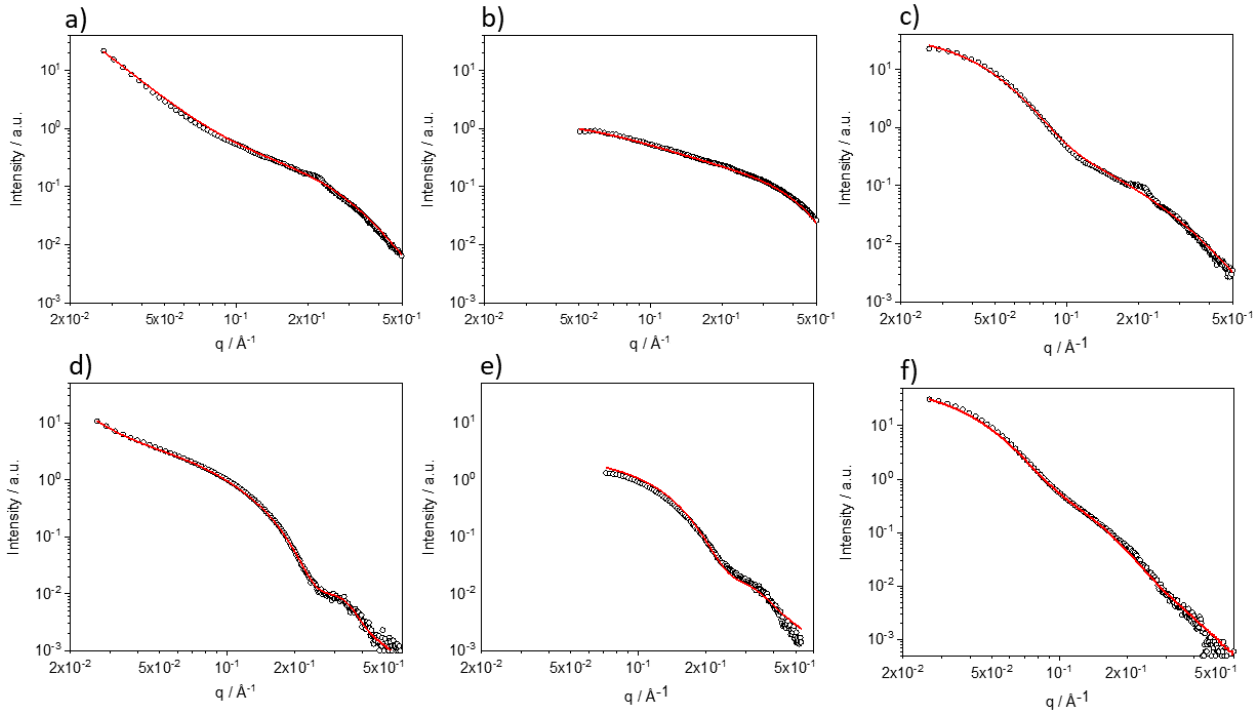

Figure S3. SAXS data and fits for the conditions before (a, b and c) and after (d, e and f) applying the degradation test. (a, d) monometallic Pt/C NPs, (b, e) Pt-IrO_2/C nanocomposite and (c, f) Pt-Au/C nanocomposite.

Table S1. Parameters of SAXS data fits and size analysis.

Samples		Power law		1st population			2nd population			Size and distribution							
		Ax 10^6	n	R_1 (Å)	σ_1	C_1	R_2 (Å)	σ_2	C_2	D_1	σ_1 '	D_2	σ_2 '	Average Diameter D (nm)	Standard Deviation of D σ (nm)	Volume fraction1	Volume fraction2
Pt/C	As prepared	180	3.25	8.0	0.30	0.008				1.7	0.5			1.7	0.5	1	0
	EOT	7	3.80	18.0	0.13	0.008	26.0	0.30	0.008	3.6	0.4	5.4	1.7	4.0	0.6	0.74	0.26
Pt-IrO_2/C	As prepared	0	2.30	6.1	0.17	0.015	14.0	0.50	0.005	1.2	0.2	3.2	1.7	1.3	0.2	0.98	0.02
	EOT	300	2.30	18.0	0.18	0.015				3.7	0.7			3.7	0.7	1	0
Pt-Au/C	As prepared	0	3.20	8.0	0.40	0.004	45.0	0.30	0.035	1.7	0.7	9.4	2.9	3.8	1.0	0.73	0.27
	EOT	20	3.00	16.0	0.25	0.003	48.0	0.30	0.038	3.3	0.8	10.0	3.0	7.0	1.7	0.45	0.55

Table S2. Particle size of the investigated catalysts before and after electrochemical measurements derived from the SAXS analysis. The standard deviation is determined from three independent measurements. BOT: before test, EOT: end of test.

		Pt/C	Pt-Au/C			Pt-IrO_2/C		
		Pt	Pt	Au	Mean size (nm)	Pt	Ir	Mean size (nm)
Particle size (nm)	BOT	1.7 ± 0.5	1.7 ± 0.7	9.4 ± 2.9	3.8 ± 1.0	3.2 ± 1.7	1.2 ± 0.2	1.3 ± 0.2
	EOT	4.1 ± 0.6	3.3 ± 0.8	10.0 ± 3.0	7.0 ± 1.7	-	-	3.7 ± 0.7

The SAXS data were recorded directly from the GDEs made from the respective catalyst by vacuum filtration. Unlike in RDE measurements no catalyst collection from multiple measurements is required as shown in our previous work[1].

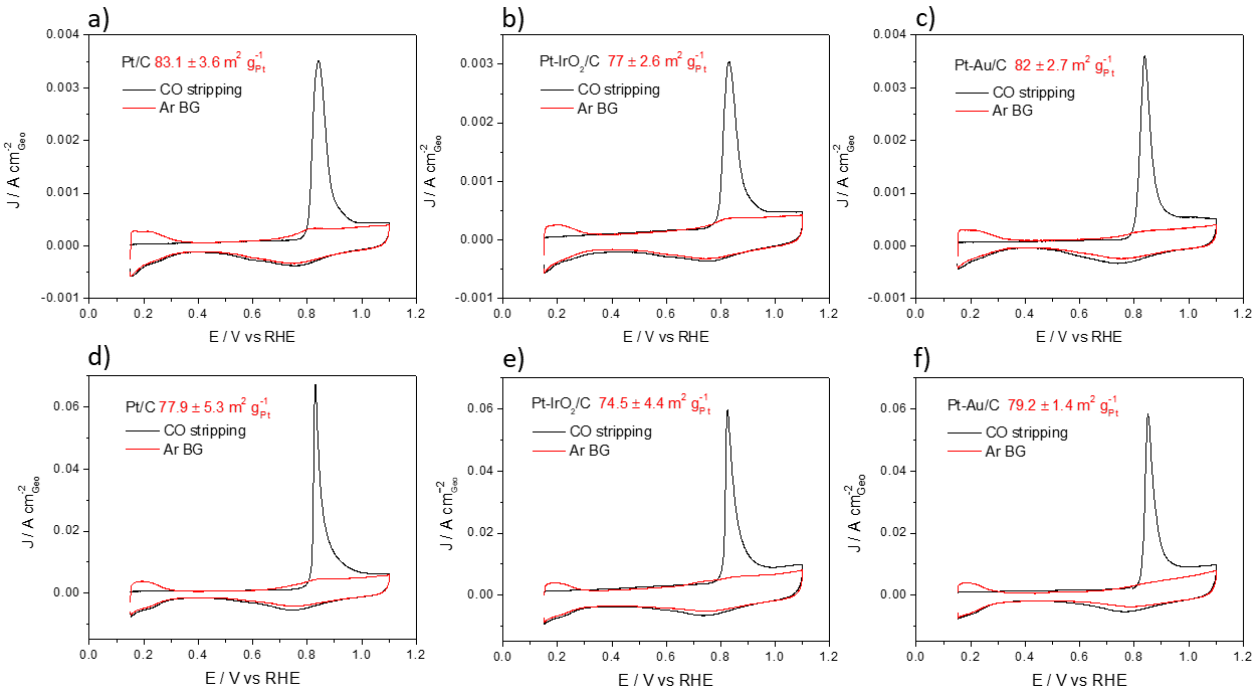

Figure S4. Representative CO stripping curves (black line) and the subsequent CVs (red line) of the monometallic Pt/C catalyst (a, d), the Pt-IrO_2/C nanocomposite (b, e) and the Pt-Au/C nanocomposite (c, f) from both RDE (a, b, c) and GDE (d, e, f) measurement approaches. The scan rate is 50 mV s^{-1}. The insert averaged ECSA value is obtained from three independent measurements from both measurement approaches. All measurements were recorded at room temperature in $HClO_4$ aqueous electrolyte.

The single CO oxidation peak can be taken as an indication that no Pt NP agglomeration is apparent in the as-prepared catalysts. The Pt surface area of the corresponding catalysts measured by the GDE approach is slightly lower than that determined by the RDE approach (Figure S4), we assume that the Nafion in catalyst ink for the GDE measurements is mainly responsible for this difference (Nafion is not added to the catalyst ink for the RDE measurement) as a portion of Pt active sites might be blocked by Nafion and the specific adsorption of sulphonate groups from Nafion on the Pt surface must also be taken into account[2,3]. The difference, however, is small. The largest determined difference in Pt area between RDE and GDE measurements is 6% (20 wt.% Pt/C).

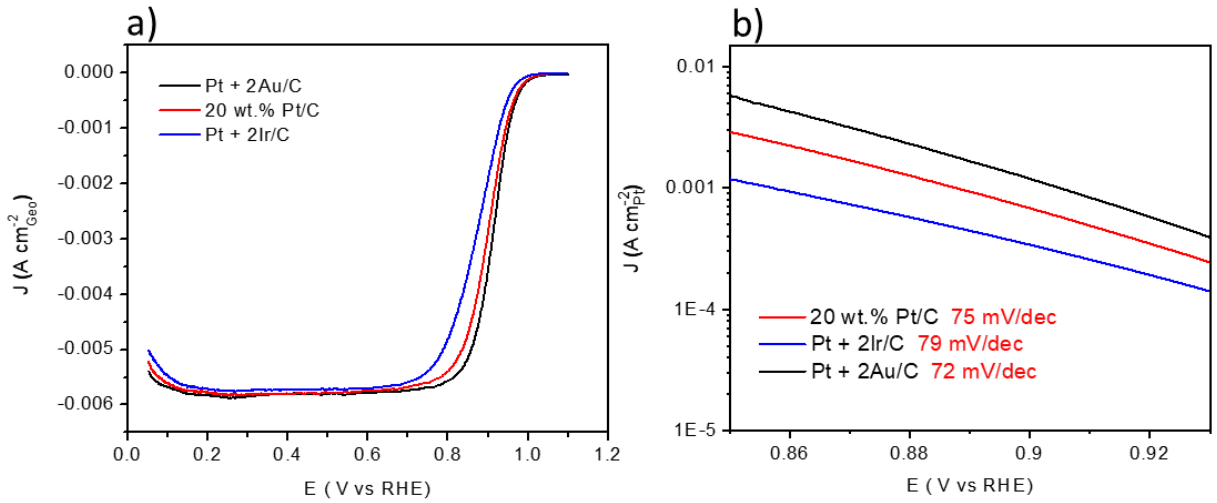

Figure S5. Comparison of linear sweep voltammograms (positive scans) of the investigated catalysts (a) and the Tafel plots extracted from the linear sweep voltammograms (b). The measurements were conducted in O_2 saturated 0.1 M $HClO_4$ aqueous electrolyte with a scan rate of 50 mV s^{-1} at room temperature. The obtained linear sweep voltammograms were corrected by Ar background and solution resistance.

The averaged polarization curves from three independent measurements are displayed in Figure S5a, these polarization curves are obtained from positive scan direction in O_2 saturated 0.1 M $HClO_4$ and after Ar background correction. We can see that the current density increases in the order of Pt + 2Ir/C to 20 wt.% Pt/C to Pt + 2Au/C in the mixed of kinetic-diffusion controlled

region (0.75-1.00 V_{RHE}) which is normally used to determine ORR performance. Tafel plots are extracted from these polarization curves and depicted in Figure S5b, we can see that the Tafel plots are basically parallel to each other.

Table S3. ORR performance of the investigated catalysts from RDE and GDE approach. The ORR activity is determined at the potential of 0.85 V_{RHE} and from negative scan direction of the respective polarization curve from RDE approach. The standard deviation is determined from three independent measurements.

		Pt/C	Pt-IrO_2/C	Pt-Au/C
RDE	$SA_{0.85\ V}$ ($\mu A\ cm_{Pt}^{-2}$)	915 ± 58	416 ± 16	1280 ± 102
	$MA_{0.85\ V}$ ($A\ g_{Pt}^{-1}$)	750 ± 63	307 ± 26	1060 ± 71
GDE	$SA_{0.85\ V}$ ($\mu A\ cm_{Pt}^{-2}$)	81.8 ± 7.8	23.1 ± 2.8	107 ± 8.7
	$MA_{0.85\ V}$ ($A\ g_{Pt}^{-1}$)	63.7 ± 6.9	17.2 ± 3.1	85.1 ± 6.2

As seen, the absolute ORR activity in the RDE measurements is higher than the one determined in the GDE measurements (Table S3). This difference is related to several factors: i) a different catalyst ink composition (the ink for the GDE measurements contains Nafion while the one for the RDE measurement does not Nafion). This is also consistent with the lower ECSA obtained from the GDE measurements as compared to the RDE measurements. Nafion is known to partially block Pt active sites, and therefore insufficient Pt utilization is observed.[3] According to previous reports, an increase in the Nafion content improved the catalyst performance up to a Nafion weight percentage of 20% by Xu et al[4], while a decreased performance can be observed when the Nafion content is above 20 wt.%, same phenomenon was reported by Kim et al[5], who found 25 wt.% of Nafion content yielded the best performance in ORR activity. In our case, the Nafion content is in a range between 36 wt.% and 44 wt.% (the weight ration of Nafion/carbon is 1 in each catalyst), excess Nafion is possible to result in a suboptimal performance of the investigated catalysts in

ORR activity if referring to the above results. ii) even if ORR activity evaluation from RDE is selected from negative scan polarization curve, it is still possible to overestimate the ORR activity as a partial transient activity might contribute to the overall ORR rate evaluation from RDE measurement. iii) the configuration of the cell body from RDE and GDE approach are completely different, which can also be a source for activity deviation.

Table S4. ECSA obtained from CO stripping measurement before and after degradation test and the corresponding ECSA loss from both RDE and GDE measurement approach. Four different degradation protocols were applied for stability determination in RDE measurement while a mixed degradation protocol was applied in GDE measurement. The measurement results of Pt/C and Pt-IrO_2/C based on current mode protocol are resued from reference [6]. The standard deviation is determined from three independent measurements. BOT: before test, EOT: end of test.

Catalysts / Stability			Pt/C	Pt-IrO_2/C	Pt-Au/C
RDE ECSA (m^2 g_{Pt}^{-1})	BOT	0.6 V-1.6 V	85.6 ± 3.0	77.5 ± 2.9	86.1 ± 1.9
		1.0 V-1.5 V	81.7 ± 1.6	79 ± 1.2	82.5 ± 4.1
		0.4 V-1.4 V	84.8 ± 0.5	76.6 ± 4.1	82.7 ± 4.5
		Current mode	83.1 ± 3.6	77 ± 2.6	84.5 ± 1.7
	EOT	0.6 V-1.6 V	53.1 ± 1.3	49.2 ± 2.0	54.8 ± 1.3
		1.0 V-1.5 V	58.4 ± 1.3	65.2 ± 0.8	66 ± 2.7
		0.4 V-1.4 V	29.9 ±1.8	32.7 ± 2.3	27.2 ± 2.4
		Current mode	51.5 ± 3.4	61.9 ± 3.6	64.4 ± 4.8
Loss %	0.6 V-1.6 V		37.9 ± 0.7	36.5 ± 0.8	36.4 ± 0.5
	1.0 V-1.5 V		28.5 ± 1.0	17.5 ± 0.6	19.9 ± 2.5
	0.4 V-1.4 V		64.7 ± 2.1	57.4 ± 1.6	67.2 ± 1.1
	Current mode		38.1 ± 1.4	19.6 ± 1.3	23.7 ± 4.6
GDE ECSA (m^2 g_{Pt}^{-1})	BOT		77.9 ± 5.3	74.5 ± 4.4	79.2 ± 1.4
	EOT		52.3 ± 1.6	51.8 ± 2.0	60.2 ± 3.7
Loss %			32.9 ± 3.9	30.5 ± 4.3	24 ± 2.2

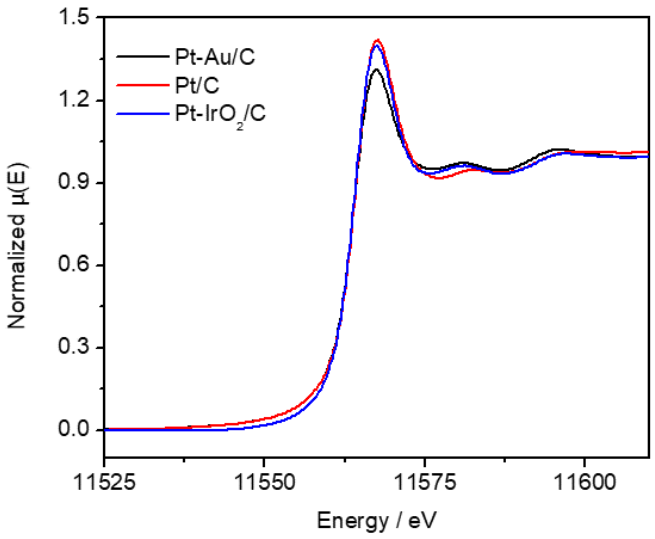

Figure S6. Normalized Pt L_3-edge XANES spectra of the supported monometallic Pt NPs and nanocomposite of Pt-Au/C and Pt-IrO_2/C.

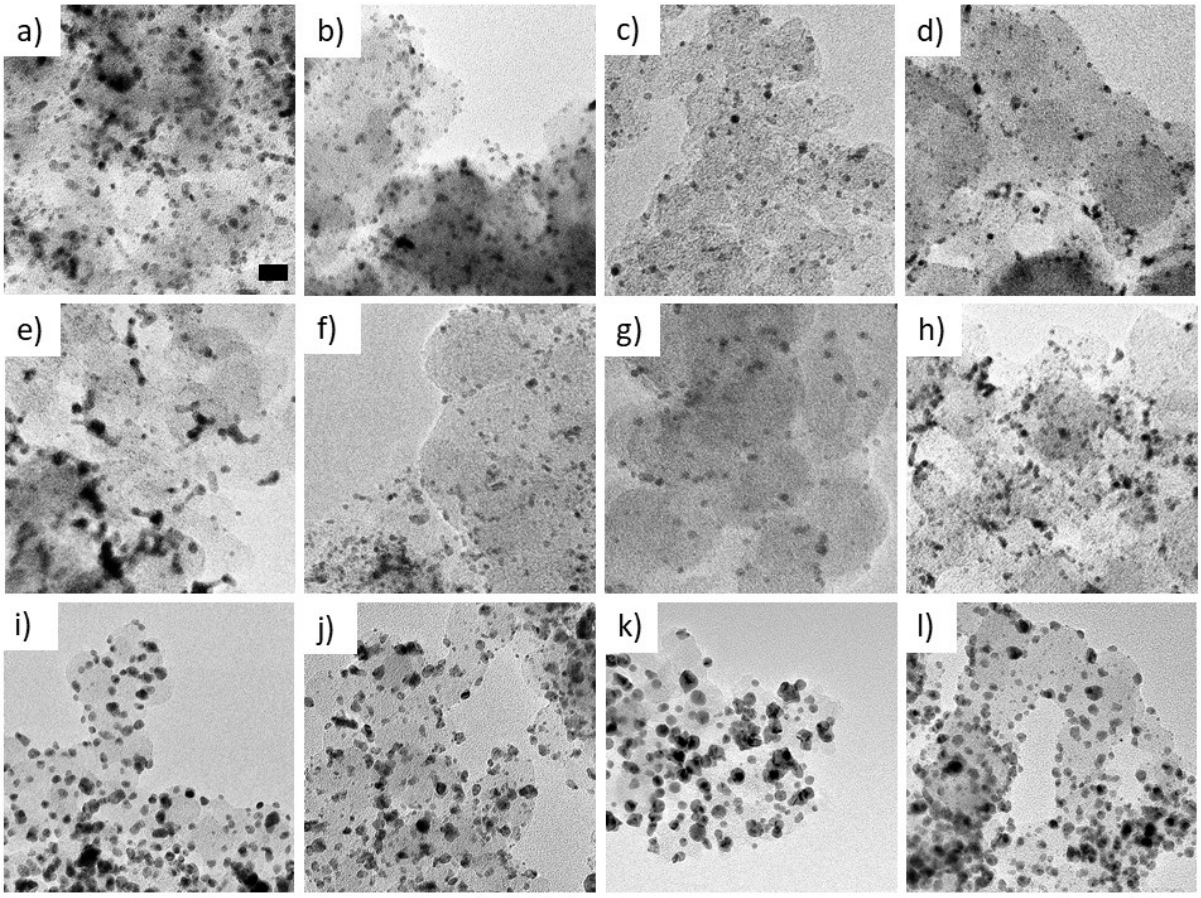

Figure S7. TEM micrographs recorded at the same magnification of the degraded catalysts with RDE approach. (a, b, c and d) Nanocomposite of Pt-IrO_2/C, (e, f, g and h) Supported monometallic Pt NPs and (i, j, k and l) Nanocomposite of Pt-Au/C. (a, e and i) are the degraded catalysts after subject to the degradation protocol as schemed in Figure S2a, (b, f and j) are the degraded catalysts after subject to the degradation protocol as schemed in Figure S2b, (c, g and k) are the degraded catalysts after subject to the degradation protocol as schemed in Figure S2c and (d, h and l) are the degraded catalysts after subject to the degradation protocol as schemed in Figure S2d. The scale bar for given in (a) is the same for all micrographs and is 20 nm.

Table S5. Weight compositions of Ir, Au and Pt that determined from TEM-EDX (RDE) and SEM-EDX (GDE). The calculated weight ratio before and after ADTs of each supported nanocomposite is obtained from five independent measurements. BOT: before test, EOT: end of test.

			Ir or Au wt. %	Pt wt. %	Ir/Pt or Au/Pt
RDE	Pt-IrO_2/C	BOT	67.0 ± 0.7	33.0 ± 0.7	2.03
		0.6 -1.6 V	34.0 ± 6.7	66.0 ± 6.7	0.52
		1.0 V-1.5 V	49.0 ± 18.7	51.0 ± 18.7	0.96
		0.4 V-1.4 V	40.0 ± 10.0	60.0 ± 10.0	0.67
		Current mode	32.0 ± 17.0	68.0 ± 17.0	0.47
	Pt-Au/C	BOT	66.0 ± 1.3	34.0 ± 1.3	1.95
		0.6 V-1.6 V	63.0 ± 2.8	37.0 ± 2.8	1.70
		1.0 V-1.5 V	69.0 ± 13.8	31.0 ± 13.8	2.23
		0.4 V-1.4 V	70.0 ± 13.6	30.0 ± 13.6	2.33
		Current mode	66.0 ± 4.2	34.0 ± 4.2	1.94
GDE	Pt-IrO_2/C	BOT	67.4 ± 2.0	32.6 ± 2.0	2.10
		EOT	49.7 ± 0.8	50.3 ± 0.8	0.99
	Pt-Au/C	BOT	65.5 ± 0.6	34.5 ± 0.6	1.90
		EOT	64.6 ± 0.7	35.4 ± 0.7	1.80

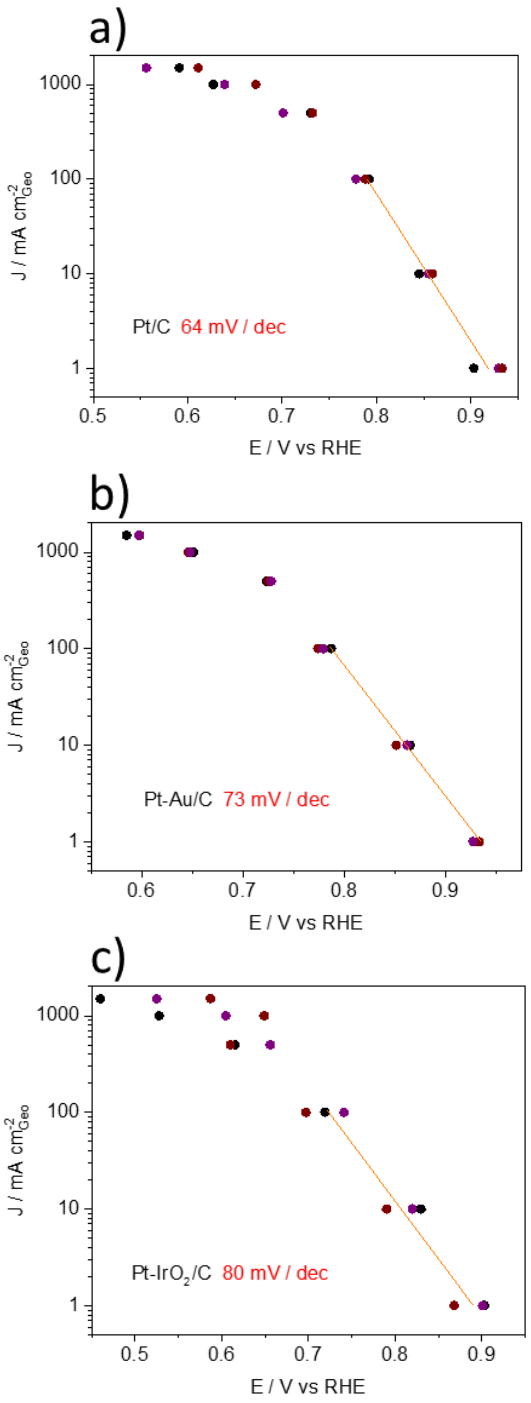

Figure S8. ORR performance before degradation test with GDE approach of supported monometallic Pt NPs (a), nanocomposite of Pt-Au/C (b) and Pt-IrO_2/C (c). Three independent measurement results are displayed in the corresponding figure, the recorded dots with the same color are from the same measurement. The current density is presented in logarithmic form. The Tafel slope is estimated from the first three measurement results.

References

(1) Schröder, J.; Quinson, J.; Mathiesen, J. K.; Kirkensgaard, J. J. K.; Alinejad, S.; Mints, V. A.; Jensen, K. M. Ø.; Arenz, M. A New Approach to Probe the Degradation of Fuel Cell Catalysts under Realistic Conditions: Combining Tests in a Gas Diffusion Electrode Setup with Small Angle X-Ray Scattering. *Journal of The Electrochemical Society* **2020**. https://doi.org/10.1149/1945-7111/abbdd2.

(2) Velázquez-Palenzuela, A.; Centellas, F.; Brillas, E.; Arias, C.; Rodríguez, R. M.; Garrido, J. A.; Cabot, P. L. Kinetic Effect of the Ionomer on the Oxygen Reduction in Carbon-Supported Pt Electrocatalysts. *International Journal of Hydrogen Energy* **2012**, *37* (23), 17828–17836. https://doi.org/10.1016/j.ijhydene.2012.09.090.

(3) Kodama, K.; Shinohara, A.; Hasegawa, N.; Shinozaki, K.; Jinnouchi, R.; Suzuki, T.; Hatanaka, T.; Morimoto, Y. Catalyst Poisoning Property of Sulfonimide Acid Ionomer on Pt (111) Surface. *Journal of The Electrochemical Society* **2014**, *161* (5), F649–F652. https://doi.org/10.1149/2.051405jes.

(4) Xu, W.; Scott, K. The Effects of Ionomer Content on PEM Water Electrolyser Membrane Electrode Assembly Performance. *International Journal of Hydrogen Energy* **2010**, *35* (21), 12029–12037. https://doi.org/10.1016/j.ijhydene.2010.08.055.

(5) Kim, K. H.; Lee, K. Y.; Kim, H. J.; Cho, E. A.; Lee, S. Y.; Lim, T. H.; Yoon, S. P.; Hwang, I. C.; Jang, J. H. The Effects of Nafion® Ionomer Content in PEMFC MEAs Prepared by a Catalyst-Coated Membrane (CCM) Spraying Method. *International Journal of Hydrogen Energy* **2010**, *35* (5), 2119–2126. https://doi.org/10.1016/j.ijhydene.2009.11.058.

(6) Du, J.; Quinson, J.; Zhang, D.; Bizzotto, F.; Zana, A.; Arenz, M. Bifunctional Pt-IrO2 Catalysts for the Oxygen Evolution and Oxygen Reduction Reactions: Alloy Nanoparticles versus Nanocomposite Catalysts. *ACS Catalysis* **2021**, *11* (2), 820–828. https://doi.org/10.1021/acscatal.0c03867.